ORIGINAL PAPER

Dry Fractionation and Crystallization Kinetics of High-Oleic High-Stearic Sunflower Oil

**Miguel A. Bootello · Rafael Garcés ·
Enrique Martínez-Force · Joaquín J. Salas**

Abstract Fractionation of fats and oils makes it possible to generate products with specific properties from natural fats that contain a variety of triacylglycerol (TAG) species. High-oleic high-stearic (HOHS) sunflower oils contain high levels of saturated fatty acids, mainly stearate, on a high-oleic background. Accordingly, HOHS oils could be a source of disaturated TAGs appropriate for cocoa butter equivalent formulations. We examined the kinetics of HOHS oil crystallization, paying special attention to the influence of crystal seeding and temperature on the process and the composition of the final fractions. This oil was fractionated at 18 °C, and seeding increased the amount of disaturated TAGs recovered in the precipitate from 23% to up to 30%. The experimental data collected were fitted using the models of Gompertz and Avrami to study how well these models fitted the data and their utility in predicting the progress of crystallization. At seeding additions above 0.25% there was a change in the crystallization mechanism that improved the process of fractionation. The effect of temperature was also studied, showing important increases in the maximum rates of crystallization when fractionations were carried out at lower temperatures. Finally, the melting profiles of the fractions enriched in saturated fatty acids were studied, showing amounts of solids intermediate between the initial oil and cocoa butter.

M. A. Bootello · R. Garcés · E. Martínez-Force · J. J. Salas (✉)
Instituto de la Grasa (CSIC), Av. Padre García Tejero 4,
41012 Seville, Spain
e-mail: jjsalas@cica.es

Introduction

Natural vegetable fats and oils are complex mixtures of triacylglycerols (TAGs), the composition of which depends on the species from which they have been extracted [1]. Liquid vegetable oils rich in unsaturated fatty acids, such as soybean, canola, cotton or olive oils, are usually refined and retailed without any additional processing. However, fats rich in saturated fatty acids, such as those from palm or palm kernel, usually contain a wider variety of TAG species that are associated with broader melting intervals and which are not appropriate for retail or industrial use [2]. Thus, these fats are usually fractionated so that the TAGs with different melting points can be separated by crystallization. Each crystallization step yields a solid fraction or stearin and a liquid fraction or olein, which can then be further fractionated to produce fractions with even more well-defined melting profiles and potential uses [3]. The best known fractionation process is that used for palm oil [4], a multistep process involving crystallization and high pressure filtration of stearins. This process separates fractions enriched in trisaturated, disaturated, and polyunsaturated TAGs that can be employed for different uses.

Advances in oilseed breeding and biotechnology have made the production of new oils enriched in saturated fatty acids possible [5, 6]. These oils and fats have a composition that differs from those traditionally used as the source for plastic fats or in the preparation of confectionery products, highlighting the need for studies into the most appropriate methods for their fractionation [2, 7].

🌢 Springer AOCS❖

High-oleic high-stearic (HOHS) sunflower lines produce sunflower oils rich in stearic acid while retaining the high levels of oleic acid in their TAG molecules. This oil can be fractionated in the presence of hexane to produce stearins enriched in stearic acid, which have improved physical properties for production of healthy and valuable cocoa butter equivalents (CBEs) [8]. While solvent fractionation is an efficient method to produce high-melting-point stearins, the high costs associated with managing large amounts of solvent make dry fractionation the preferred method in industry.

Fat crystallization is the determinant step in fractionation, involving two steps: nucleation and crystal growth. Nucleation is the process during which the first stable crystals are formed in the overcooled mixture of melted TAGs [9]. This can be a homogeneous process if nuclei are formed spontaneously by direct interaction between the most saturated TAG molecules. Alternatively, nucleation may be heterogeneous when the process takes place on the surface of particles or the walls of the container in contact with the suspension. Once nuclei are formed, they can grow by incorporating TAG molecules from the liquid phase into the crystalline network. The rate and pattern of crystal growth will depend on factors such as the degree of overcooling and the diffusion rate of the crystallizing molecules from the liquid phase [10]. During this process, latent heat of crystallization is liberated and must be removed from the system for correct crystal formation. Crystal growth will stop when the concentration of the most saturated TAGs reaches their solubility constant in the liquid matrix at the temperature of fractionation [11].

In this work, the kinetics of HOHS sunflower oil crystallization was studied by monitoring the size of the apparent crystalline fraction (F_c) formed from HOHS oil over time at different temperatures, and by evaluating the effect of adding seeding crystals. Two models of crystallization kinetics were applied to this system to account for the effects on nucleation and crystal growth: the models of Avrami [12] and Gompertz [13]. Applying these models, a parameterized equation that reflected the progress of

crystallization was defined, and information regarding the mechanism of crystallization was obtained. Furthermore, the stearins and oleins resulting from fractionation were characterized, paying special attention to the enrichment of disaturated TAGs in the stearins when compared with the initial oil (those with the general formula saturated–unsaturated–saturated, SUS). The melting interval of these fractions was also studied by differential scanning calorimetry (DSC) to define their potential applications in the elaboration of confectionery products.

Experimental Methods

Materials

Refined, bleached, deodorized, and partially dewaxed HOHS sunflower oil was provided by Nutrisun Business as the starting material (see TAG composition in Table 1). This oil is commercially available at http://www.nutrisunoil.com.

Oil Fractionation

HOHS sunflower oil was melted at 80 °C to remove any previous structure, then fractionated in a 1-L thermostated glass reactor connected to a 1157P programmable temperature controller (VWR International, USA) with mild agitation (30 rpm). The high-melting-point stearins used to produce seeding crystals were prepared by solvent fractionation as described by Salas et al. [8]. These stearins accounted for 74.5% of disaturated TAGs (Table 1), and they were grated and sieved to maximum particle size of 1.6 mm. When HOHS sunflower oil reached the fractionation temperature, the high-melting-point stearin powder was added and the kinetic studies began.

The progress of oil fractionation was monitored by removing 5-mL samples at different times. To obtain fractions for later fatty acid and TAG analysis, they were filtered using a small Büchner funnel and a Kitasato flask connected to a portable vacuum pump N86KT-18 (Neuberg

Table 1 Triacylglycerol composition of the high-oleic high-stearic (HOHS) sunflower oil and the seeding stearin used in this work

	Triacylglycerols (% w/w)													
	POP	POSt	POO	POL	StOSt	StOO	OOO	StOL	OOL	OLL	StOA	OOA	StOB	OOB	SUS
HOHS oil	0.3	2.2	7.2	1.0	4.2	32.5	31.9	5.2	5.6	0.7	0.7	2.8	0.7	4.2	8.1
Seeding stearin	0.4	7.5	2.0	0.1	51.0	9.7	9.7	0.8	1.2	0.1	7.0	0.8	8.7	1.3	74.5

Triacylglycerols are denoted by three symbols; corresponding to the fatty acids esterified at positions 1, 2 and 3. Peaks accounting for <0.1% of total triacylglycerols were not integrated. Data represent averages of two independent determinations

P palmitic, *O* oleic, *St* stearic, *L* linoleic, *A* arachidid, *B* behenic, *SUS* total disaturated triacylglycerol

Laboport, Freiburg, Germany). Vacuum filtration of the final stearins was carried out when the olein composition was constant over time. This step was performed using a filtration system similar to that described previously but using a jacketed 1-L filtering plate to maintain the fractionation temperature constant during the entire operation, since dry fractionation filtration is slower than solvent fractionation. The final stearins were washed with five volumes of hexane at 5 °C to remove the rest of the occluded olein.

TAG Analysis by GLC

The TAG composition of the different oil fractions was determined by gas–liquid chromatography (GLC) in an Agilent 6890 gas chromatograph (Palo Alto, CA) equipped with a Quadrex aluminum-clad 400-65HT chromatography column (30 m length, 0.25 mm i.d., 0.1 μm film thickness; Woodbridge, CT, USA) and a flame ionization detector (FID). Hydrogen was used as the carrier gas at linear gas rate of 50 cm s^{-1} and split ratio of 1:80. The injector and detector temperatures were 360 and 370 °C, respectively, the oven temperature was 335 °C, and a head pressure gradient from 100 to 180 kPa was applied. The relative response of the FID was corrected according to the method of Carelli and Cert [14].

Analysis of Fatty Acid Methyl Esters

The fatty acid composition was determined by GLC, derivatizing 5 mg of the oil fractions to their corresponding fatty acid methyl esters for 1 h at 80 °C with 1.5 mL methanol/toluene/sulfuric acid (88/10/2, v/v/v). Fatty acid methyl esters were extracted with 1 mL heptane and analyzed by GLC on an Agilent 6890 gas chromatography system (Palo Alto, CA) equipped with a Supelco SP-2380 fused-silica capillary column (30 m length; 0.25 mm i.d.; 0.20 μm film thickness: Bellefonte, PA, USA), using hydrogen as the carrier gas at 28 cm s^{-1}. The detector and injector temperature were 200 °C, whereas the oven temperature was kept at 170 °C. The different methyl esters were identified by comparison with known standards.

Calorimetric Analysis by DSC

The melting profiles of the different oils and oil fractions were determined by differential scanning calorimetry (DSC) using a Q2000 V23.5 scanner (TA instruments, New Castle, DE, USA). The results were processed using the TA analysis software provided by the manufacturer. This instrument was calibrated prior to use with metallic indium (melting point 156.6 °C, $\Delta H_f = 28.45$ J g^{-1}). Samples were prepared by pipetting 6–8 mg of the melted oils and oil fractions into

aluminum pans, and weighing them using a Sartorius M2P electronic microbalance (Sartorius AG, Goettingen, Germany). The pans were then sealed and balanced calorimetrically, using an empty sealed capsule as the reference.

To study the melting profiles, samples were kept at 90 °C for 10 min to destroy any previous structure, then cooled to 0 °C for 30 min and kept at 5 °C over 24 h. Finally, the samples were transferred to an oven at 26 °C for 48 h. Each sample was loaded into the calorimeter at 20 °C, and the temperature was quickly decreased to −40 °C before being increased to 90 °C at a rate of 1 °C min^{-1}.

The solid fat content (SFC) was determined by continuous integration of the DSC melting curves using the TA universal analysis software.

Data Analysis

The progress of crystallization was assessed on the basis of the 1,3-stearoyl-2-oleoyl glycerol (StOSt) balance, as this species of triacylglycerol is of special interest since it would be the main component of a CBE produced from these oils. The StOSt composition of the oleins over time reflects the progress of crystallization, and the stearin crystal mass at time t can be calculated as the balance of StOSt according to the following equation:

$$M_c = \frac{M_0\,(\%\mathrm{StOSt}_0 - \%\mathrm{StOSt}_t^{\mathrm{Olein}})}{\%\mathrm{StOSt}^{\mathrm{Stearin}} - \%\mathrm{StOSt}_t^{\mathrm{Olein}}}, \tag{1}$$

where M_c is the stearin crystal mass at time t (g), M_0 is the initial oil mass (g), $\%\mathrm{StOSt}_0$ is the StOSt concentration in the initial oil (% w/w), $\%\mathrm{StOSt}_t^{\mathrm{Olein}}$ is the StOSt concentration in olein at time t (% w/w), and $\%\mathrm{StOSt}^{\mathrm{Stearin}}$ is the StOSt concentration in the final stearin (% w/w).

From these data, the apparent fraction of crystals in the suspension at time t can be obtained as

$$F_c = \frac{M_c}{M_0}. \tag{2}$$

The F_c versus time data can be used in crystallization models such as those of Avrami [12] and Gompertz [13]. The isothermal crystallization kinetics of HOHS sunflower oil was evaluated by the Avrami equation

$$(1 - F_c) = \exp\{-kt^n\}, \tag{3}$$

where F_c is the fraction of the crystal transformed at time t during crystallization, k is the rate constant, and n is the Avrami exponent related to the crystallization mechanism. This equation can be expressed in logarithmic form as

$$\ln[-\ln(1 - F_c)] = \ln k + n \ln t. \tag{4}$$

The values of n and k were obtained from the slope and y-intercept of a plot of $\ln[-\ln(1 - F_c)]$ versus $\ln t$. The

Avrami parameters provide information on the nature of the crystallization process. The constant k represents a crystallization rate constant, and the Avrami exponent n indicates the mechanism of crystal growth. Nucleation is either instantaneous, with nuclei appearing all at once early on in the process, or sporadic, with the number of nuclei increasing linearly over time [15]. Growth can be linear (one dimension), plate-like (two dimensions) or spherical (three dimensions). Indeed, the Avrami exponent may reflect the different types of nucleation and growth [15, 16]; for example, an exponent of $n = 1$ indicates linear growth from instantaneous nuclei, whereas $n = 2$ represents plate-like growth along two dimensions from sporadic nuclei, or one-dimensional growth from instantaneous nuclei.

The Gompertz isothermal crystallization model has been used to describe crystallization and seeding in a quantitative manner, whereby experimental data are fitted using the Gompertz equation

$$F_c = a_g \exp\left\{ -\exp\left[\frac{\mu e}{a_g}(\lambda - t) + 1 \right] \right\}, \quad (5)$$

where a_g is the maximum value for the fraction of crystal F_c, μ is the growth rate (h^{-1}), and λ is the induction time (h). Estimation of the parameter was performed by non-linear regression using OriginPro 8.0 software (OriginLab Corp., Northampton, USA).

Statistical Analysis

Fractionation and kinetics experiments were carried out in duplicate, and all the results concerning fractionation presented herein correspond to averages of the two determinations for each sample. Standard deviations not specified in the paper are presented in the Supplementary Material.

DSC diagrams represent single determination of typical fractions.

Results

Influence of Seeding According to the Gompertz Model

Crystallization assays were run isothermically at 18 °C with the addition of different hard stearin seeding crystals. The fraction of crystals in the suspension was monitored as a function of time (Fig. 1a) when the percentage of added hard stearin increased from 0% to 1% by weight. Increasing the amount of seeding stearin reduced the activation time prior to crystallization from 21.6 to 2.6 h (parameter λ in Table 2). At the same time, the parameter μ, which is associated with the maximum rate of crystallization, was reduced, ranging from 0.0038 to 0.0112 h^{-1} (Table 2). The final percentage of precipitate was also altered by seeding, and accordingly, a_g fell from 0.149 when no seeding was applied to 0.1 in all other cases. The empirical data were fitted well by the Gompertz sigmoidal kinetics, displaying squared correlation coefficients up to 0.99 for this model.

Influence of Seeding According to Avrami's Model

The data on the course of crystallization following the addition of distinct amounts of seed stearin were fitted using Avrami's model; in this case, the squared correlation coefficients ranged from 0.72 to 0.93 (Fig. 1b; Table 2). The parameters resulting from this model showed that there were two distinct of kinetic courses, one with an n coefficient close to 1 (following the addition of large amounts seeding stearin) and another with an n coefficient above 2

Fig. 1 Course of high-oleic high-stearic sunflower oil crystallization at 18 °C using different amounts of high-melting stearin powder for seeding. **a** Fit of the experimental data using the Gompertz model. **b** Fit of the experimental data using the model of Avrami. Symbols correspond to experimental data and lines to equations resulting from the application of each model. Experiments were carried out at 0% (*filled squares, solid line*), 0.05% (*filled triangles, dashed line*), 0.25% (*crosses, dash-dotted line*), 0.5% (*open circles, dash-double dotted line*), and 1% (*filled circles, dotted line*) of stearin seeding
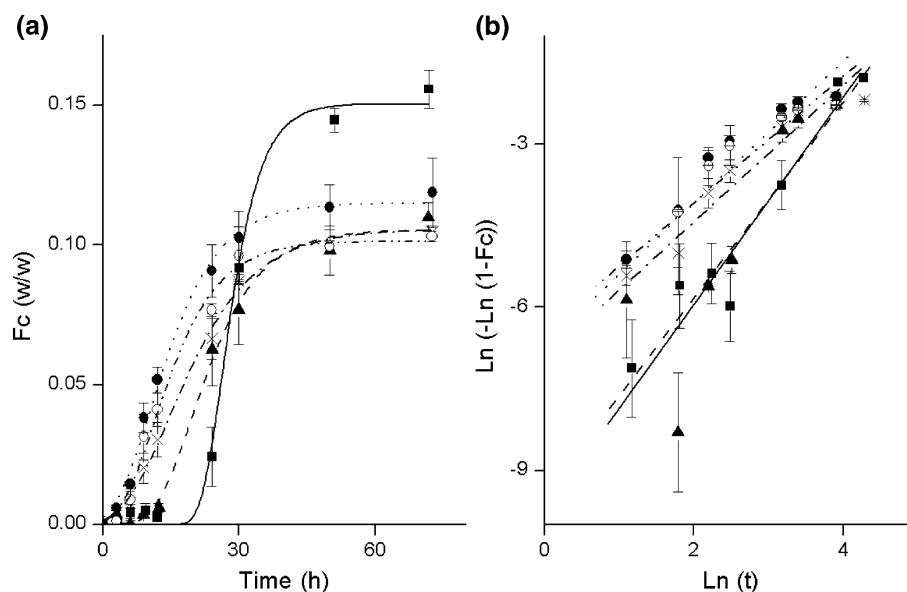
Table 2 Kinetic parameters obtained by fitting the Gompertz and Avrami models to the kinetics of crystallization (at 18 °C) of high-oleic high-stearic sunflower oil with different proportions of stearin powder

Seeding (%)	Gompertz				Avrami			
	λ (h)	μ (h^{-1})	a_g (w/w)	R^2	$n_{experimental}$	n	$k \times 10^3$ (h^{-n})	R^2
0.00	21.6 ± 1.8	0.0112 ± 0.0018	0.149 ± 0.006	0.9951	2.06 ± 0.16	2	0.045 ± 0.013	0.9198
0.05	11.5 ± 0.1	0.0048 ± 0.0011	0.106 ± 0.005	0.9949	1.88 ± 0.08	2	0.073 ± 0.002	0.7211
0.25	4.5 ± 1.0	0.0038 ± 0.0003	0.106 ± 0.002	0.9967	1.15 ± 0.04	1	1.300 ± 0.211	0.9235
0.50	3.8 ± 0.6	0.0048 ± 0.0006	0.102 ± 0.001	0.9914	0.95 ± 0.08	1	2.199 ± 0.044	0.8904
1.00	2.6 ± 0.0	0.0052 ± 0.0006	0.115 ± 0.010	0.9944	1.11 ± 0.01	1	2.411 ± 0.302	0.9258

Data represent averages of two independent determinations

(little or no stearin addition). The values of the Avrami constant k increased with the addition of stearin, ranging from 0.045×10^{-3} with no seeding to 2.411×10^{-3} h^{-n} when 1% of solid stearin powder was added to the crystallizing suspension.

Influence of Seeding on Final Composition

The fractions finally obtained by dry fractionation of HOHS sunflower oil following seeding with different percentages of high-melting-point stearin were analyzed for their TAG composition (Table 3). Addition of seeding crystals did not alter the composition of the final liquid fractions or oleins, all of which displayed similar SUS content of around 6%. However, seeding did have an impact on the composition of the stearins. Thus, the final

content of disaturated TAGs was considerably lower when no seeding occurred (23.3%), although the final yield of stearin was higher (15.5%). Addition of stearin powder increased the proportion of SUS in the final solid fraction to between 30% and 33%, albeit in association with lower final yields (10–12%).

Influence of Temperature in the Gompertz Model

The influence of temperature on fractionation was studied by applying 0.25% crystal seeding and running isothermal kinetics at 17.5, 18, and 19 °C. When the Gompertz equation was fitted to the experimental data, the squared correlation coefficients were higher than 0.99, indicating that crystallization was fitted well by sigmoidal kinetics (Fig. 2a; Table 4). Lower temperatures accelerated the

Table 3 Triacylglycerol composition of final fractions resulting from dry fractionation at 18 °C of high-oleic high-stearic oil using different proportions of stearin powder for seeding

Seeding (%)	Triacylglycerols (% w/w)															Yield (%)
	POP	POSt	POO	POL	StOSt	StOO	OOO	StOL	OOL	OLL	StOA	OOA	StOB	OOB	SUS	
Stearins																
0.00	0.5	4.6	6.6	0.5	14.2	27.2	30.7	2.6	3.3	0.7	2.0	2.0	2.0	3.1	23.3	15.5 ± 0.4
0.05	0.5	5.8	5.7	0.4	20.9	24.0	26.4	2.2	3.0	0.4	3.0	1.8	3.1	2.7	33.4	10.2 ± 0.6
0.25	0.4	5.2	5.9	0.5	19.1	24.8	27.0	2.3	3.3	0.9	2.8	1.9	3.0	2.9	30.5	11.0 ± 0.8
0.50	0.5	5.2	5.4	0.5	20.8	25.0	26.0	2.1	2.9	0.8	2.8	1.8	3.1	2.9	32.4	10.7 ± 0.4
1.0	0.5	5.3	5.5	0.4	20.5	23.9	25.6	2.4	3.4	0.9	3.0	1.9	3.6	3.2	32.8	12.4 ± 1.1
Oleins																
0.00	0.4	2.2	8.1	0.7	2.2	32.6	38.0	3.1	4.4	0.8	0.5	2.5	0.6	3.9	5.7	84.5 ± 0.4
0.05	0.4	2.2	8.3	0.7	2.3	32.5	38.1	3.1	4.4	0.7	0.4	2.5	0.8	3.5	6.1	89.8 ± 0.6
0.25	0.4	2.2	8.3	0.8	2.3	32.3	37.3	3.0	4.6	1.2	0.8	2.5	0.7	3.6	6.4	89.1 ± 0.8
0.50	0.3	2.0	7.7	0.7	2.6	33.1	37.4	3.2	4.3	0.8	0.5	2.6	0.9	4.0	6.2	89.4 ± 0.4
1.00	0.3	2.0	7.6	0.8	2.2	32.4	36.9	3.1	5.0	1.0	0.7	2.6	1.0	4.4	6.2	87.6 ± 1.1

Stearin compositions are corrected to take into account the presence of the seeding crystals, which were supposed to remain in the solid fraction. Triacylglycerols are denoted by three symbols; corresponding to the fatty acids esterified at positions 1, 2 and 3. Peaks accounting for <0.1% of total triacylglycerols were not integrated. Data represent averages of two independent determinations

P palmitic, *O* oleic, *St* stearic, *L* linoleic, *A* arachidid, *B* behenic, *SUS* total disaturated triacylglycerols

Fig. 2 Course of high-oleic high-stearic sunflower oil crystallization at different temperatures with 0.25% seeding. **a** Fit of the Gompertz model to the experimental data. **b** Fit of the Avrami model to the experimental data. Symbols correspond to experimental data, and lines correspond to equations resulting from applying each model. Experiments carried out at 17.5 °C (*filled squares, solid line*), 18 °C (*filled triangles, dashed line*), and 19 °C (*crosses, dotted line*)
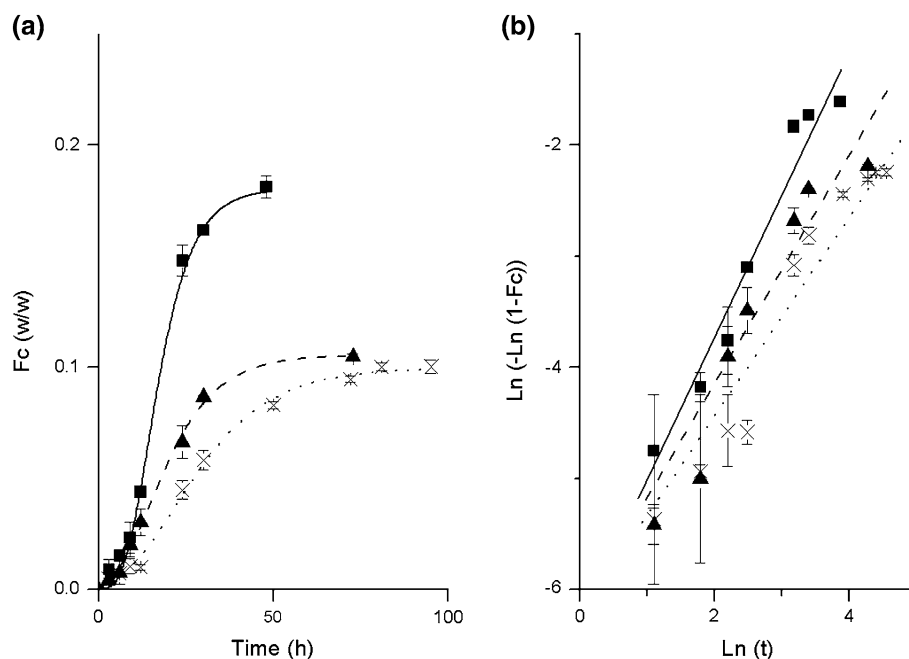
process of crystallization, giving rise to higher maximum crystallization rates (μ values). In addition, the final recovery of the solid phase also augmented at lower temperatures, ranging from 0.184 at 17.5 °C to 0.010 at 19 °C.

Influence of Temperature in the Avrami Model

The fit of the Avrami model to the dry fractionation curves at different temperatures was also assessed (Fig. 2b; Table 4). When the Avrami equation was fitted to the experimental data, the logarithmic representations gave rise to a series of lines with similar slopes, corresponding to Avrami exponent of 1. The lines corresponding to the different temperatures generated a constant k that decreased with temperature, ranging from 1.77×10^{-3} at 17.5 °C to 1.26×10^{-3} at 19 °C.

Influence of Temperature on the Composition of the Final Fraction

The temperature of fractionation also influenced the final fractions obtained after filtration of the final product.

Lower crystallization temperatures gave rise to higher stearin yields (Table 5), ranging from 17.8% to 9.4% in the temperature interval studied. This increment in yield was associated with slightly higher recovery of total SUS from the liquid phase but which diminished in the final oleins from fractionation at lower temperatures (6%), increasing to 7.2% when fractionation was performed at 19 °C. Moreover, the fractionation temperature altered the SUS content of the final stearins, which were richer in SUS when they were obtained at higher temperatures. The stearin with the highest disaturated TAG content was that obtained at 19 °C (33.9%), whereas that obtained at 17.5 °C contained 23.8% of these TAG species.

DSC Analysis of the Different Stearins

The stearins obtained by dry fractionation were analyzed by DSC, and their melting profiles were compared with those of the initial oil and of cocoa butter (Fig. 3). The percentage of solids calculated at temperatures between 25 and 40 °C was higher in the stearins containing a higher

Table 4 Kinetic parameters from the fits of the Gompertz and Avrami models to the crystallization kinetics for high-oleic high-stearic sunflower oil at different temperatures (0.25% seeding)

Temperature (°C)	Gompertz				Avrami			
	λ (h)	μ (h^{-1})	a_g (w/w)	R^2	$n_{\text{experimental}}$	n	$k \times 10^3$ (h^{-n})	R^2
17.5	6.8 ± 0.7	0.0093 ± 0.0003	0.184 ± 0.002	0.9977	1.29 ± 0.16	1	1.771 ± 8 × 10^{-4}	0.9603
18.0	4.5 ± 1.0	0.0038 ± 0.0003	0.106 ± 0.001	0.9967	1.15 ± 0.04	1	1.300 ± 0.211	0.9235
19.0	6.7 ± 1.3	0.0025 ± 0.0000	0.010 ± 0.010	0.9981	1.02 ± 0.12	1	1.264 ± 7 × 10^{-4}	0.9551

Data represent averages of two independent determinations

Table 5 Triacylglycerol composition of the final fractions resulting from dry fractionation of high-oleic high-stearic sunflower oil at different temperatures and 0.25% seeding

Temperature (°C)	Triacylglycerols (%, w/w)															Yield (%)
	POP	POSt	POO	POL	StOSt	StOO	OOO	StOL	OOL	OLL	StOA	OOA	StOB	OOB	SUS	
Stearins																
17.5	0.5	4.6	6.6	0.6	13.9	26.7	29.5	2.4	4.0	0.9	2.3	2.1	2.5	3.4	23.8	17.8 ± 0.5
18.0	0.4	5.2	5.9	0.5	19.0	24.9	27.1	2.3	3.3	0.9	2.8	1.9	3.0	2.9	30.4	10.9 ± 0.8
19.0	0.5	5.6	5.7	0.5	21.5	23.5	25.6	2.1	3.0	1.0	3.1	1.8	3.1	2.8	33.9	9.4 ± 0.7
Oleins																
17.5	0.4	2.1	8.1	0.7	2.3	32.5	36.8	3.2	4.9	1.0	0.7	2.5	0.7	4.0	6.2	82.2 ± 0.5
18.0	0.4	2.2	8.3	0.8	2.3	32.3	37.3	3.0	4.6	1.2	0.8	2.5	0.7	3.6	6.4	89.1 ± 0.8
19.0	0.4	2.3	8.1	0.8	2.6	31.9	36.5	2.9	4.9	1.4	1.0	2.4	0.9	3.8	7.2	90.6 ± 0.7

Stearin compositions are corrected to account for the presence of the seeding crystals, which were supposed to stay in the solid fraction
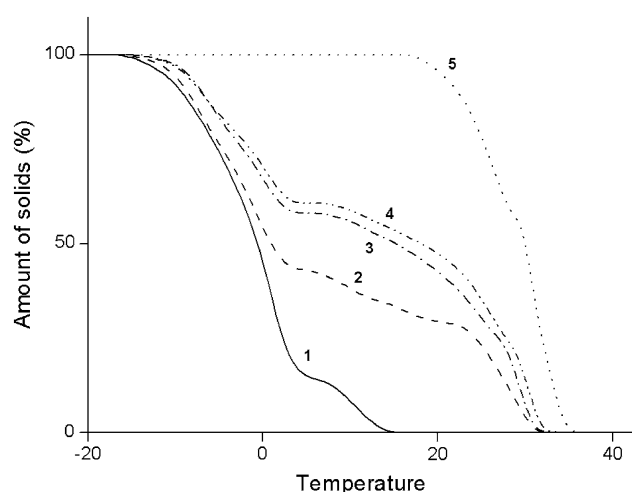

Fig. 3 Melting profiles obtained by differential scanning calorimetry of high-oleic high-stearic oil (1, *solid line*) and different stearins obtained by dry fractionation of the oil. These stearins accounted for 23.8% (2, *dashed line*), 30.4% (3, *dash-dotted line*), and 33.9% (4, *dash-double dotted line*) of disaturated triacylglycerols. The melting profile of cocoa butter (5, *dotted line*) is also presented

proportion of disaturated TAGs. Moreover, there were more solids than in the initial oil, although there were far less solids than observed in cocoa butter (CB).

Discussion

Dry fractionation of fats rich in saturated fatty acids has become important industrially, making large-scale production of a broad variety of fatty food products possible, mainly from palm and palm kernel oils. Although the conditions under which fats rich in either palmitic or lauric fatty acids can be fractionated industrially have been well defined, there is little information about dry fractionation of oils rich in stearic acid. HOHS sunflower oil is a source of stearic-acid-rich disaturated TAGs such as StOSt,

appropriate for CBE formulation (Table 1). Thus, it was possible to produce high-melting-point stearins from such oil by solvent fractionation with hexane [8]. However, this is an expensive process in terms of initial and operational costs, and thus, dry fractionation is the preferred method to produce fractions enriched in saturated fatty acids industrially, avoiding the need to add solvents to the initial oil. Therefore, the possibility of using dry fractionation to obtain high-melting-point stearins from HOHS sunflower oil was studied in this work. The most important step in this process involves induction of selective crystallization of the most saturated TAGs present in the initial oil, allowing them to be separated by physical means.

The main kinetic aspects of the fat crystallization studied were the impact of adding seeding nuclei and the temperature of fractionation. The progress of crystallization was monitored as a function of the F_c in the suspension, which was calculated by filtering the crystal suspension and analyzing the fractions obtained at different times. The apparent percentage of crystallized fat was determined as the balance of disaturated TAGs in the resulting fractions, and the experimental data obtained were fitted using the Gompertz and Avrami models.

Seeding was achieved by adding a powder of high-melting-point stearin produced by hexane fractionation [8]. This stearin contains up to 75% SUS and is stable in suspension when added to HOHS oil at the temperatures used for crystallization. Preliminary studies of HOHS oil fractionation using 16.5% of stearic acid indicated that the temperature interval at which crystallization occurs is relatively narrow. Thus, at temperatures below 17 °C the crystalline fraction was too large and difficult to filter, while at temperatures above 19 °C very few filterable crystals were produced. Thus, the seeding assays were run at 18 °C, where the addition of increasing amounts of seeding crystals altered the pattern of crystallization in the HOHS sunflower oil.

The Gompertz model allows the kinetics of crystallization to be parameterized in terms of the activation time (λ), maximum crystallization rate (μ), and the final proportion of crystallized fat (a_g) [17]. The fit of this model to the experimental data was excellent, and in all cases, the squared correlation coefficient was always as high as 0.99 (Fig. 1a; Table 2). When no seeding was applied, the induction times were longer, giving rise to higher λ values. Furthermore, the maximum rate of crystallization (μ) was the highest. This kinetic profile indicated that the time necessary to form nuclei increased the activation time when no seeding was applied, but once formed, they induced more rapid formation of crystallized fat. This phenomenon may reflect the larger number of active nuclei in such conditions than in the other assays. In such circumstances, the final amount of crystallized fat was also maximal, although it contained the lowest proportion of SUS. This compromise is consistent with the lower specificity of crystallization when growth is based on a large number of nuclei that yield elevated proportions of smaller crystals that are difficult to filter. Adding larger amounts of seeding crystals induced lower λ and μ values, as well as decreased stearin content despite the higher SUS content (Table 3). A similar amount of disaturated TAGs was found in the final olein fractions, indicating that the final recovery of these TAG species from the initial oil was independent of seeding. Thus, we conclude that the addition of high-melting-point stearin powder for seeding does not change the total time required for crystallization (Fig. 1a), but rather, it made this process more selective. Accordingly, stearins with higher saturated fatty acid contents can be produced, being easier to filter. It is also notable that the Gompertz model very closely described the progress of HOHS oil crystallization in isothermal conditions and thus could serve to simulate this process accurately for future industrial scaling.

The changes in the mechanism of crystallization induced by seeding are better described by fitting the model of Avrami to the experimental data. This model was initially used for crystallization of metals, and it is theoretically based on spherical growth of crystal nuclei [18]. However, the Avrami equation has already been successfully applied to other systems such as oils and fats [19, 20]. This model describes crystallization through the index of crystallization n, whereas the Avrami constant k is a function of the nucleation and crystallization rates [15]. The fit of the Avrami equation to the experimental data resulted in two groups of lines depending on the percentage of seeding crystals added. The kinetics in the absence of seeding, or when little seeding stearin is added, produces lines with slopes twice those found in experiments with a higher proportion of seeding. The Avrami parameters were obtained for each fit, and experiments run at 0% and 0.05%

seeding displayed Avrami coefficients close to 2, a value that corresponds to a mechanism based on spontaneous nucleation and linear crystal growth. By contrast, the exponents for higher seeding proportions grouped around a value of 1, in agreement with a mechanism based on instantaneous nucleation and linear growth. This means that the amount of seeding stearin necessary to induce a change in the mechanism of crystallization is between 0.05% and 0.25%. Moreover, the Avrami constant k increased with addition of more seeding stearin.

The influence of temperature on the crystallization of HOHS sunflower oil was studied by monitoring the kinetics of crystallization at three temperatures within the range where specific crystallization was possible; 0.25% of seeding stearin was shown to be the minimum amount that influenced crystallization. The Gompertz and Avrami models were fitted to the experimental data, and according to the parameters resulting from the former model, no differences in activation time were found (Table 4), probably due to the consistent use of seeding. However, temperature exerted a clear influence on the final crystal content of the suspension (a_g) and on the crystallization rate (μ). Thus, at lower crystallization temperatures, the amount of precipitate recovered increased from 9.4% at 19 °C to 17.8% at 17.5 °C (Table 5), and so did the rates, which ranged from 0.0025 to 0.0093 h^{-1} (Table 4). When the Avrami equation was fitted to the experimental data, the temperature appeared not to induce a change in the mechanism within the range studied, since the Avrami exponent was the same in all experiments. By contrast, the Avrami constant increased at lower crystallization temperatures. With regard to the composition of the final fractions, the stearin yield was inversely proportional to the SUS content (Table 5). Thus, these TAGs accounted for 23.8% of the precipitate obtained at 17.5 °C, increasing to 33.9% at 19 °C. Furthermore, the SUS content was lower in oleins resulting from fractionation at lower temperatures, indicating that the recovery of high-melting-point TAGs in the stearin was greater when crystallization was run at these conditions.

In studying the crystallization kinetics of HOHS sunflower oil, we assessed the melting profiles of the resulting stearins by DSC and compared them with those of CB (Fig. 3). Indeed, the amount of solid stearins obtained by dry fractionation in the temperature range from 15 to 30 °C reflected their content of disaturated TAG species. Unlike CB, all sunflower stearins displayed broad melting intervals, and the fractions containing higher proportions of SUS had higher solid content, although not as high as the solid content of CB. In this regard, the stearins obtained by dry fractionation contain less disaturated TAGs than most stearins obtained by solvent fractionation [8], and thus, they contained less solids at the temperatures studied here.

Nevertheless, these results indicate that a single step of dry fractionation is insufficient to produce stearins with a melting profile similar to that of CB, although it could be useful to enrich the initial oil in disaturated TAGs, which could be interesting within a multistep industrial process.

Conclusions

It was possible to fractionate HOHS sunflower oil without the addition of any solvents. The crystallization kinetics could be monitored and fitted well by the Gompertz and Avrami models. The addition of high-melting-point stearin powder induced changes in the nucleation mechanism, decreasing the total time and the selectivity of crystallization, which improved the performance of filtration and the fractionation process as a whole. To improve this process, between 0.05% and 0.25% w/w seeding stearin had to be added, and fractionation was also influenced by temperature. The range of temperatures for which disaturated TAGs were specifically precipitated was narrow, and lower temperatures accelerated the rates of crystallization and increased the recovery of disaturated TAGs from the initial oil. By contrast, higher temperatures gave rise to stearins enriched in saturated fatty acids. Stearins yielded by dry fractionation of HOHS oils have broad melting profiles and cannot be used for CBE formulation. However, dry fractionation of that oil is efficient in producing fractions enriched in saturated fatty acids and could be used to produce different fat products (structured fats, spreads), or as an intermediate step in production of high-melting-point stearins appropriate for confectionery fat formulation.

References

1. Garcés R, Martínez-Force E, Salas JJ, Venegas-Calerón M (2009) Current advances in sunflower oil and its applications. Lipid Technol 21:79–82

2. Salas JJ, Bootello MA, Martínez-Force E, Garcés R (2009) Tropical vegetables fats and butters: properties and new alternatives. OCL Oleagineaux 16:254–258

3. Timms RE (2005) Fractional crystallization–the fat modification process for the 21st century. Eur J Lipid Sci Technol 107:48–57

4. Kellens M, Gibon V, Hendrix M, De Greyt W (2007) Palm oil fractionation. Eur J Lipid Sci Technol 109:336–349

5. Pleite R, Martinez-Force E, Garces R (2006) Increase of the stearic acid content in high-oleic sunflower (*Helianthus annuus*) seeds. J Agric Food Chem 54:9383–9388

6. Fernández-Moya V, Martínez-Force E, Garcés R (2005) Oils from improved high stearic acid sunflower seeds. J Agric Food Chem 53:5326–5330

7. Dubinsky E (2008) Utilización de aceites de girasol alto esteárico como alternativa saludable en la industria de alimentos. Aceites y Grasas 71:352–358

8. Salas JJ, Bootello MA, Martínez-Force E, Garcés R (2011) Production of stearate-rich butters by solvent fractionation of high stearic-high oleic sunflower oil. Food Chem 124:450–458

9. Metin S, Hartel RW (2005) Crystallization of fats and oils. In: Shahidi F (ed) Bailey's Industrial oil and fat products, 6th edn, vol 6. Wiley, London

10. Timms RE (1997) Fractionation. In: Gunstone FD (ed) Lipid technologies and applications. Marcel Dekker, New York

11. Sato K (2001) Crystallization behavior of fats and lipids—a review. Chem Eng Sci 56:2255–2265

12. Chong CL (2001) Crystallization of palm oil products. In: Widlak N, Hartel RW, Narine S (eds) Crystallization and solidification properties of lipids. AOCS, Champaign

13. Zwietering MH, Jongenburger I, Rombouts FM, Van't Riet K (1990) Modeling of the bacterial growth curve. Appl Environ Microbiol 56:1875–1881

14. Carelli AA, Cert A (1993) Comparative study of the determination of triacylglyceride in vegetable oil using chromatographic techniques. J Chromatogr 630:213–222

15. Marangoni AG (2005) Crystallization kinetic. In: Marangoni AG (ed) Fat crystal network. Marcel Dekker, New York

16. Foubert I, Dewettinck K, Vanrolleghem PA (2003) Modelling crystallization kinetics of fats. Trends Food Sci Technol 14:79–92

17. Vanhoutte B, Dewettinck K, Foubert I, Vanlerberghe B, Huyghebaert A (2002) The effect of phospholipids and water on the isothermal crystallization of milk fat. Eur J Lipid Sci Technol 104:490–495

18. Avrami M (1939) Kinetics of phase change I: general theory. J Chem Phys 7:1103–1112

19. Metin S, Hartel RW (1998) Thermal analysis of isothermal crystallization kinetics in blends of cocoa butter with milk fat or milk fat fractions. J Am Oil Chem Soc 75:1617–1624

20. Ng GL, Oh CH (1994) Kinetic study on isothermal crystallization of palm oil by solid fat content measurements. J Am Oil Chem Soc 71:1135–1139